energies

MDPI

Article

An Operation Strategy of ESS for Enhancing the Frequency Stability of the Inverter-Based Jeju Grid

Jin-Yong Jung [1], Yoon-Sung Cho [1,*], Jae-Hyun Min [2] and Hwachang Song [3]

[1] School of Electronic and Electrical Engineering, Daegu Catholic University, Gyeongsan 38430, Korea; jjy778132@gmail.com
[2] System Planning Department, KEPCO, Naju-si 58322, Korea; jaehyun7912@kepco.co.kr
[3] Department of Electrical and Information Engineering, Seoul National University of Science and Technology, Seoul 01811, Korea; hcsong@seoultech.ac.kr
* Correspondence: philos@cu.ac.kr

Abstract: As environmental pollution deteriorates, the acceleration of decarbonization worldwide is underway. Several countries, including Korea, are incorporating new and renewable energy into existing systems, and various methods of decarbonization are being researched. With changes in the control environment, the expansion of the system linkage of new and renewable energy can cause system instability problems. This paper introduces an operation plan that uses the fast response characteristics of energy storage system(s) (ESS) to improve stability and review system stability as a result of the expansion of new and renewable energy on Jeju Island. Frequency stability was ensured through an analysis of frequency response characteristics in the event of a system accident, and an efficient ESS operation plan was simulated by changing the ESS parameters. Through this simulation, stable ESS operation and hunting in the frequency recovery process were minimized through cooperation between the existing and new ESS via a wide dead-band range and speed adjustment rate correction, and the lowest frequency was improved.

Keywords: ESS; frequency stability; renewable energy; HVDC; coordinated control

Citation: Jung, J.-Y.; Cho, Y.-S.; Min, J.-H.; Song, H. An Operation Strategy of ESS for Enhancing the Frequency Stability of the Inverter-Based Jeju Grid. *Energies* **2022**, *15*, 3086. https://doi.org/10.3390/en15093086

Academic Editors: Marcin Wołowicz, Piotr Krawczyk and Krzysztof Badyda

Received: 16 March 2022
Accepted: 19 April 2022
Published: 22 April 2022

1. Introduction

Countries are highlighting the importance of renewable energy (e.g., by expanding new and renewable energy for decarbonization) due to continuous environmental pollution problems. According to the "Renewable Energy 3020" policy, the proportion of new and renewable energy centered on wind and photovoltaics (PV) is increasing in Korea. As shown in Table 1, renewable energy and inverter-based generators are on the rise, while synchronous generators are on the decline. The 9th Basic Electricity Supply and Demand Plan intends to reduce synchronous generators such as nuclear power plants and coal power plants while increasing new and renewable energy [1]. Renewable energy in the inverter-based Jeju grid is expected to increase to 2.0 GW in 2022, 4.2 GW in 2030, and 4.4 GW in 2034. Following the above new renewable energy expansion policy, new and renewable energy input with high volatility and intermittence will increase in the future power system, and the power system will be operated stably due to the characteristics of new and renewable energy sources linked to asynchronous generators based on power electronic converters. This may cause difficulties.

Due to the renewable energy growth rate, various studies are being conducted on power system stability. Research is being conducted on new and renewable energy modeling, the development of an optimal reinforcement plan for power facilities, the development of new and renewable energy grid connection standards, and the analysis of stability (voltage/transient/frequency) for various scenarios. In terms of stability, case studies of renewable energy dropouts due to system failure are being used to analyze and correct set values (momentary cessation function, etc.) of facilities installed in new and renewable energy complexes.

Table 1. The 9th basic plan for long-term electricity supply and demand [1].

Year	Division	Coal	LNG	RE	PSH	ETC	HVDC	Total
2022	Capacity (MW)	-	480	1996	-	106	600	3182
	Ratio (%)	-	15.1	62.7	-	3.3	18.9	100
2030	Capacity (MW)	-	480	4230	-	136	600	5446
	Ratio (%)	-	8.8	77.7	-	2.5	11.0	100
2034	Capacity (MW)	-	480	4456	-	136	600	5672
	Ratio (%)	-	8.5	78.6	-	2.3	10.6	100

Regarding future systems with increased input ratios of new and renewable energy, when large-scale generators fail or output fluctuations occur due to reduced system inertia, there is the possibility of a system collapse due to a sharp drop in the system frequency before the reserve resource operates. Countermeasures must be put in place to ensure the system's stability. With the increase in renewable energy, the power system environment is changing, and studies are being conducted to prepare for it [2–5]. Concerning a recent grid accident in Korea, it was discovered that when a large-scale generator dropout occurs and the frequency is outside of the normal range, sunlight can be dropped from the grid based on the low-frequency operation setting the value of the inverter connected to the sunlight.

Recently, various studies on frequency stability improvement, according to the expansion of new and renewable energy, have been conducted. First, the North American Electric Reliability Corporation (NERC) and the North American ISO examined the frequency stability decline and system status as a result of the increased use of new and renewable energy [6–8]. To ensure frequency stability, research is being conducted to improve frequency stability using fast frequency response (FFR). In the event of a system failure, increasing the lowest frequency with additional primary reserve is insufficient. To ensure frequency stability, the frequency must be improved using the FFR's high-speed response.

Reduction of synchronous generators and expansion of inverter-based renewable energy may reduce synchronous engine inertia, decrease system robustness, and weaken dynamic stability. The drop in synchronism inertia may affect the lowest frequency drop and the rate of change of frequency (RoCoF) [6]. Figure 1 shows the frequency response characteristics according to the change in the inertia of the synchronizer. Because the low inertia system has fewer synchronous generators, the synchronous inertia decreases, RoCoF increases, and the lowest frequency decreases, as illustrated in Figure 1. Although there may be some differences depending on governor droop and new and renewable energy frequency control characteristics, the minimum frequency may be lowered due to the decrease in synchronism, the reduction in synchronism inertia, and the reduction of the effect of governor droop. RoCoF can be expressed as "$\simeq 1/\text{System Inertia}$" as "$df/dt$".

Second, research on governor droop adjustment and critical inertia calculation, according to the expansion of new and renewable energy, are in progress. UK NGESO operates the system through daily inertial monitoring based on real system data. Figure 2 shows the frequency response when the grid inertia decreases due to the increase in inverter-based generators and the frequency response according to the change of the grid reserve. The Grid Modernization Laboratory Consortium (GMLC) of the United States has tested the frequency stability contribution method using a new and renewable energy inverter, but it is still in the early stages of development. In this case, the inertia of the synchronous generator must be used to contribute to stability. RoCoF can be calculated using inertia and the severity of an accident (amount of dropout). Because of the high RoCoF, the time to reach the lowest frequency may be shortened in the event of an accident. The degree of accident occurrence, synchronous engine inertia, system reserve, and governor droop, are all important factors in frequency response.

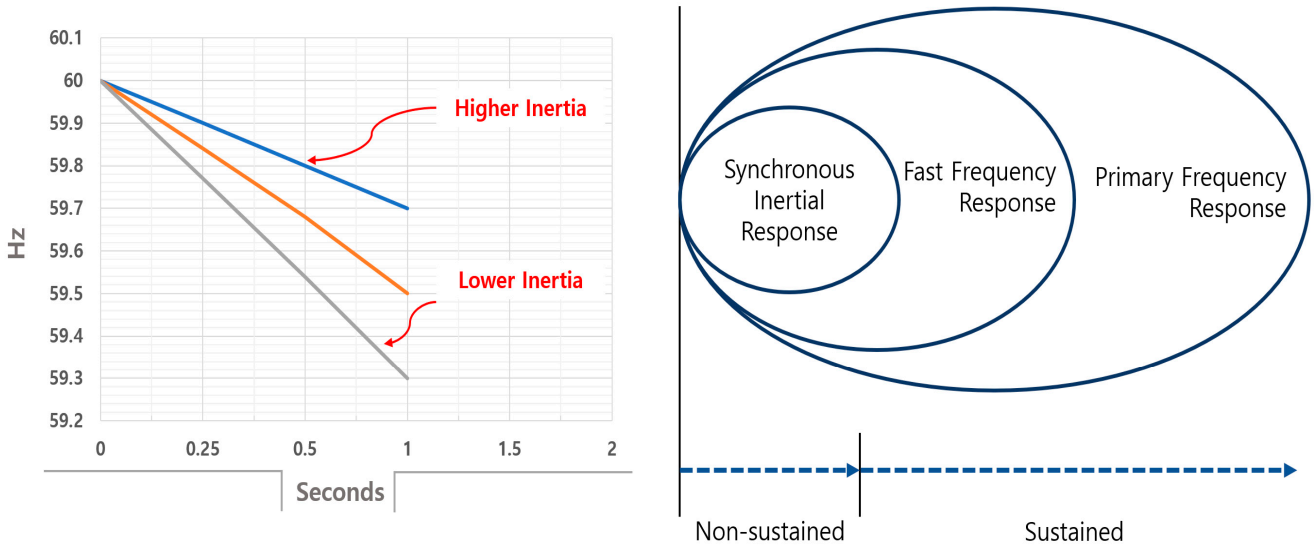

(**a**) (**b**)

Figure 1. (**a**) Frequency response characteristics according to synchronous inertia change. (**b**) Frequency response contribution of inertia; FFR—fast frequency response; PFR—primary frequency response [6].

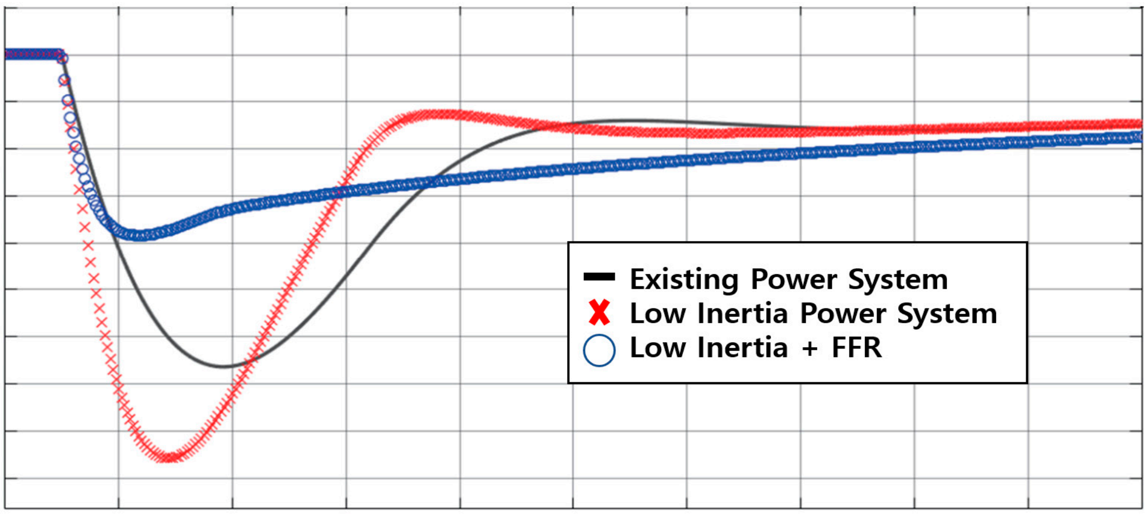

Figure 2. Frequency response according to the change of system inertia constant and reserve force [6].

In the case of domestic (Korean) grids, establishing measures to secure stability due to the expansion of new and renewable energy power generation facilities input, the intensification of uncertainty in the construction of power facilities, and the concentration of demand, are required. In particular, if the proportion of new and renewable energy is high, step-by-step countermeasures for grid stabilization are required. Stabilization measures include the use of an energy storage devices, the input of a synchronous generator, and the establishment of a net copper reserve. Among these are the need to expand ESS (Energy Storage System(s)) facilities for grid stabilization and develop detailed operational plans to alleviate power generation constraints and maintain grid reliability in future systems. As renewable energy increases, many ESS are connected to power systems to supplement the characteristics of renewable energy and are used as a way to improve frequency stability.

Many research findings on the improvement of frequency stability using ESS have shown that RoCoF is reduced and the frequency nadir is improved when grid connected ESS [9–11]. In addition, ESS had a better effect on frequency stability improvement than the governor-free mode of operation of synchronous generators [9]. Moreover, use of ESS is cheaper when compared to the cost of including inertia constraints into the unit commitment; moreover, generators will not solely be committed for the purpose of inertia, which is already given by the energy storage system [10]. Depending on the operation strategy, ESS can improve economic benefits and grid stability, and can be used as countermeasures against the volatility of new and renewable energy. For this reason, ESS have become very important power facilities in nano grids and micro grids. In addition, as research on the economic operations and life extension of ESS is in progress, greater effects can be seen in terms of economic and grid stability [5].

The inverter-based Jeju grid is a small-scale power system, and frequency response characteristics are easily changed due to changes in ESS output. To examine the frequency stability of a small-scale power system in which renewable energy is injected, this paper introduces an optimal operation and control strategy plan for securing stability after simulating frequency stability using ESS for frequency adjustment in the Jeju grid. This paper aims not only to improve the frequency stability, using only the effective power output characteristics of the ESS, but also to improve the frequency nadir and recover the stable frequency by controlling the ESS power and operation by changing the ESS parameters. As a way to stabilize frequencies using ESS in small-scale power systems, such as Jeju grids, this paper introduces stable frequency recovery by minimizing the oscillation of frequency recovery as well as the frequency nadir rise due to the increase in ESS power, dead band, droop, and exit control. This paper's ESS control strategy can contribute to the improvement of stable ESS output power and frequency stability in small-scale power systems, including Jeju grids.

2. Modeling and Methods

Recently, with the expansion of new and renewable energy, interest in frequency stability has increased, and various studies on frequency stability improvement are in progress. The Jeju grid is linked to a large amount of new and renewable energy, and it has the characteristics of a future system because it includes inverter-based facilities, such as ESS, facts, and high voltage direct current (HVDC), as well as various power facilities. As a result, after analyzing the characteristics of frequency response change in the case of generator failure due to a grid accident in the Jeju grid, we attempted to simulate frequency stability using ESS in this paper. According to the simulation results, the operation plan and control strategy plan were analyzed to improve the stable output and frequency stability of the Jeju grid ESS by adjusting the ESS parameters, such as the ESS control mode and droop speed. This paper seeks to explain the ESS control strategy for improving frequency stability through optimal parameters for ESS operation, such as contributing to a fast response by adjusting droop speed and improving the minimum frequency by increasing ESS output.

2.1. Frequency Stability Simulation Methods

In this simulation, the frequency response change according to the ESS parameter adjustment was analyzed for the optimal parameter analysis of ESS. The frequency response change due to the parameter change of the newly installed ESS No.2 (50 MW) was analyzed in this simulation, while the parameters of the existing ESS No.1 (40 MW) were kept constant. The following items were subjected to ESS No.2 parameter adjustments.

- ESS Droop control.
  - Droop speed.
- ESS RoCoF control.
  - Dead band.

- RoCoF for trans-state (trans-state judgement RoCoF).
- Droop for steady-state and trans-recovery.
- System H for trans-state (ESS output).

As shown in Figure 3, the simulation process analyzed the effects before and after parameter application by modifying the ESS No.2 parameters after analyzing the frequency response when a system accident occurred. Then, based on the simulation results through the modified parameters, the frequency response characteristics according to each parameter change were analyzed and the optimal parameters were derived through the heuristic method.

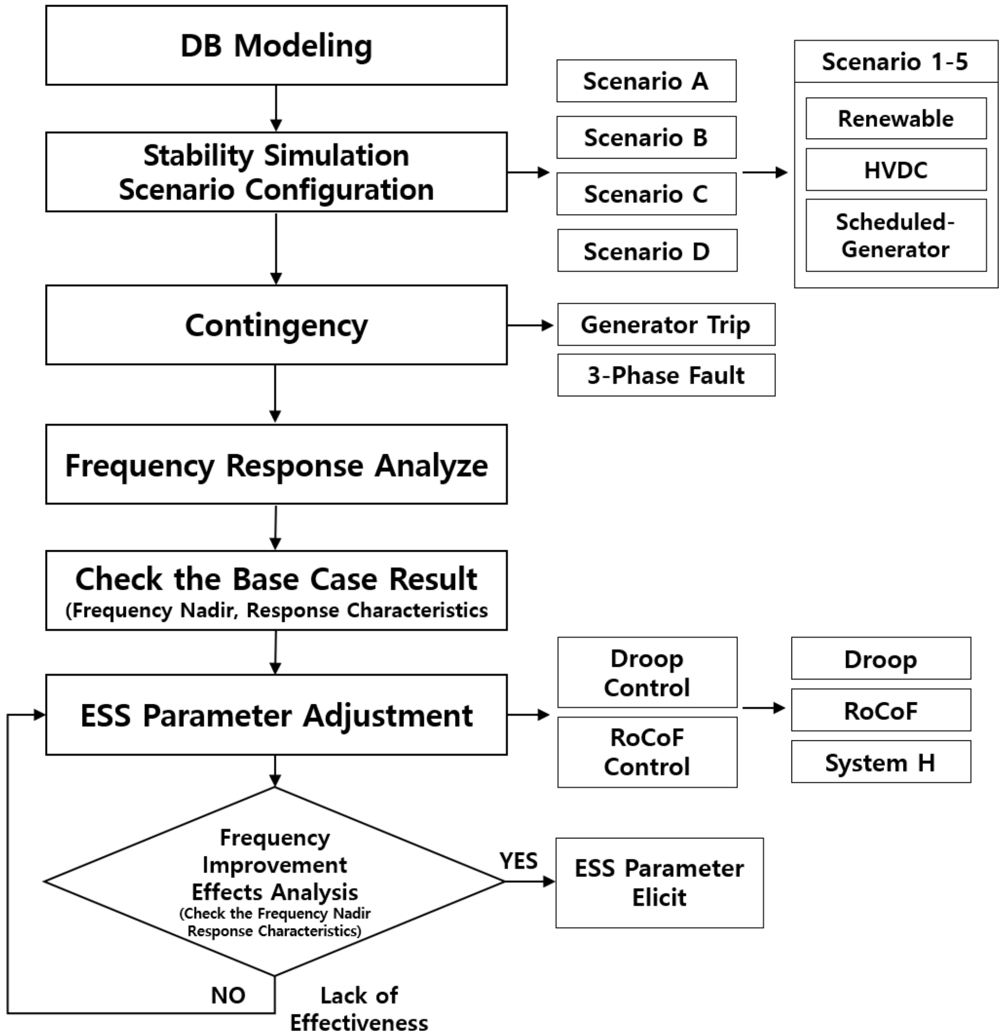

Figure 3. Simulation process.

First, scenarios 1–5 were composed according to the renewable power generation ratio and HVDC operation characteristics, and scenarios A, B, and C were classified according to the operation characteristics of HVDC No.3. Second, the system accident simulated a generator dropout and a three-phase short circuit, and the frequency response characteristics after the system accident were analyzed. The lowest frequency and oscillation occurring during the frequency recovery process were reviewed for frequency stability evaluation criteria. The reason for the oscillation review is that oscillation occurs as a result of ESS output change and repeated charging and discharging, which may be a problem in frequency stability recovery.

As shown in Figure 4, ESS parameter adjustment was performed in consideration of ESS output increase, stable output maintenance, and frequency oscillation minimization.

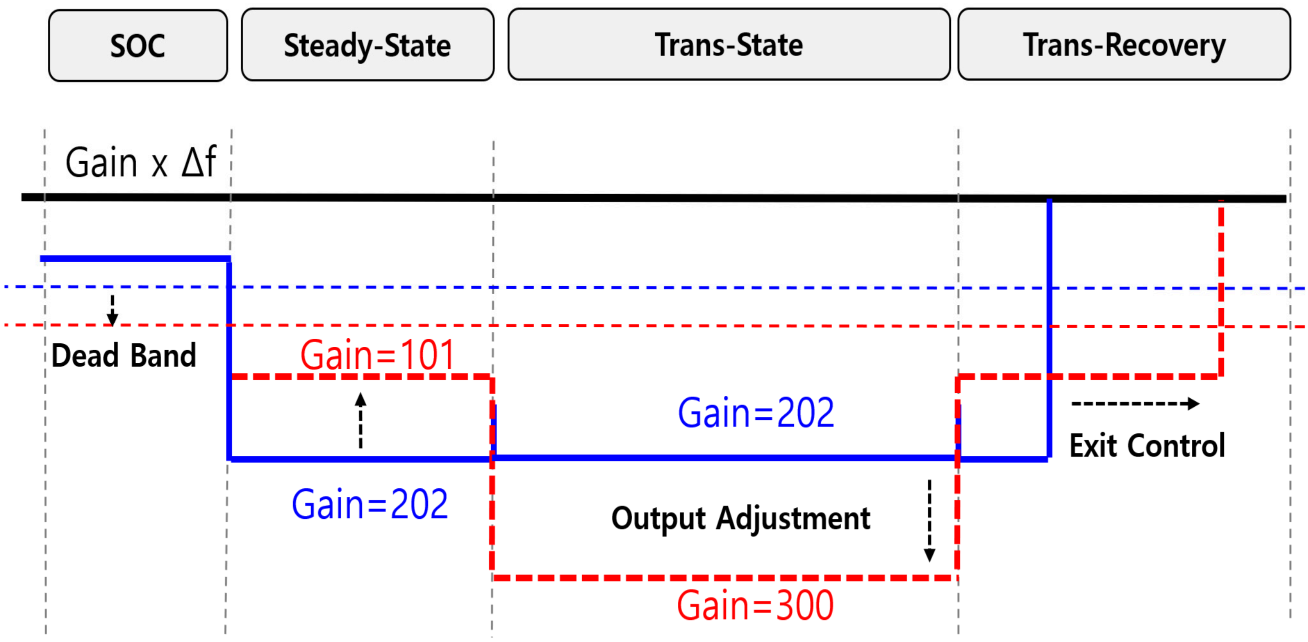

Figure 4. ESS parameter selection method.

2.2. Scenario Configuration

The database for the simulation of this thesis connected the land system and the Jeju grid, and the Jeju new and renewable energy generator and other models were modeled as shown in Table 2. For HVDC No.3 modeling, two models were analyzed—the PSS/E user defined model (UDM) and the voltage source convertor (VSC) generic HVDC, including frequency controller. After the frequency response characteristics according to HVDC modeling were analyzed, this paper used the VSC HVDC and frequency controller.

Table 2. Database configuration.

	Configuration
Wind	Company Registration Model
PV	2nd Generic Models
HVDC No.1,2	Company Registration Model
HVDC No.3	VSC and frequency controller Model
On-Shore	2022 year Database

The scenario composition for the simulation was constructed by reflecting the renewable energy and central power supply, HVDC operation characteristics, and HVDC No.3 modeling characteristics. HVDC operation characteristics are divided into forward and reverse transmission, with forward transmission referring to the amount of electricity supplied from land to Jeju and reverse transmission referring to the amount of electricity transmitted from Jeju to land. As shown in Tables 3–5, Scenarios A, B, and C are classified based on the operation characteristics and modeling of HVDC No.3. Scenarios 1 to 5 are classified according to the amount of renewable power generation for each scenario and operation characteristics of HVDC No.1,2.

- Scenario A,B,C: classification according to HVDC No.3 operation characteristics and the model.
- Scenario 1–5: classification according to the renewable power generation and HVDC circulation operation.
- Five must-run generators.

Table 3. Scenario A configuration (HVDC No.3 non-modeling).

Scenario	Load (MW)	Renewable		HVDC No.1,2		Scheduled Generator
		Wind (MW)	PV (MW)	Supply (MW)	Transmission (MW)	
1	1059	0	0	400	0	665
2	874	83	305	230	0	259
3	596	128	226	50	50	243
4	596	148	296	60	160	256
5	596	129	226	40	70	273

Table 4. Scenario B configuration (HVDC No.3 supply).

Scenario	Load (MW)	Renewable		HVDC No.1,2,3		Scheduled Generator
		Wind (MW)	PV (MW)	Supply (MW)	Transmission (MW)	
1	1059	0	0	500	0	566
2	874	84	281	260	0	250
3	596	129	141	150	50	225
4	596	129	245	160	160	224
5	596	129	171	140	70	225

Table 5. Scenario C configuration (HVDC No.3 transmission).

Scenario	Load (MW)	Renewable		HVDC No.1,2,3		Scheduled Generator
		Wind (MW)	PV (MW)	Supply (MW)	Transmission (MW)	
1	1059	0	0	350	100	768
2	874	200	340	160	100	277.6
3	595.7	218.6	231	50	150	250
4	595.7	128.5	241.4	30	170	368
5	595.7	218.6	261.4	40	170	252.4

2.3. ESS Modeling

The ESS used in this simulation comprised the PSS/E user-defined model (UDM). Figure 5 shows the ESS modeling example based on the PSS/E UDM. The ESS connection method was the connection to the connecting bus using a generator and a transformer through generator modeling, and modeling was focused on the frequency regulation (FR) ESS configuration method and power management system (PMS) applied in Korea.

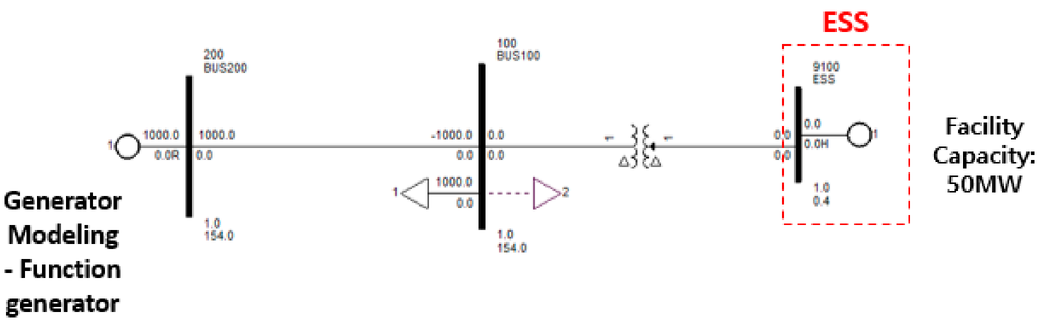

Figure 5. ESS Modeling Example.

As shown in Figure 6 the ESS operation was controlled, divided into the following four areas, by determining RoCoF after frequency acquisition:

- SOC control: control within the dead band, output, or nonoutput, according to the droop speed.
- Steady-state control: when the dead band is reached, the frequency change rate is limited to the set value, and the output is determined by the droop speed.
- Trans-state control: control when the frequency change rate exceeds the set value after exceeding the dead band; maximum output with constant system applied.
- Trans-recovery control: in the transient state, the frequency increases, and when the increased time exceeds the set value, control, and output, according to the speed adjustment rate.

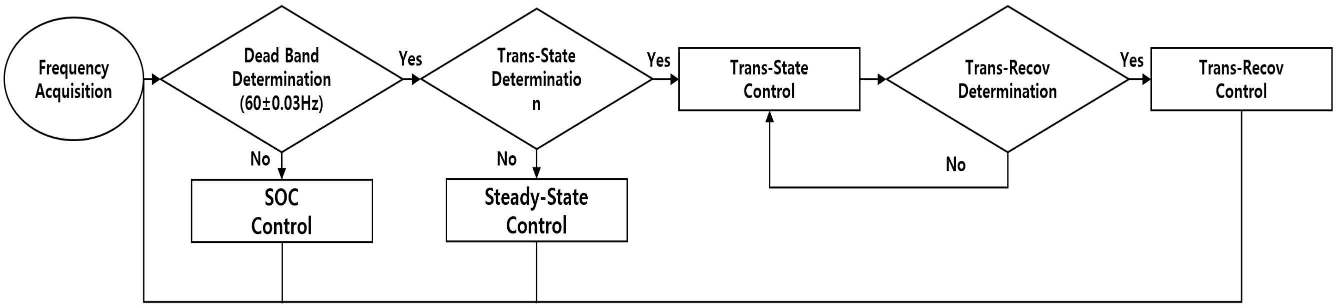

Figure 6. ESS modeling structure.

2.4. Renewable Energy Modeling

In this paper, renewable generator modeling was constructed through equivalent models mainly used overseas, such as WECC and NREL. The structure of the generator model was referred to through Appendix B. As shown in Figure 7 the equivalent model consists of a renewable generator, generator step-up (GSU) transformer equivalent transformer, collector system equivalent, a point of interest (POI) transformer, an interconnection transmission line, and plant reactive support.

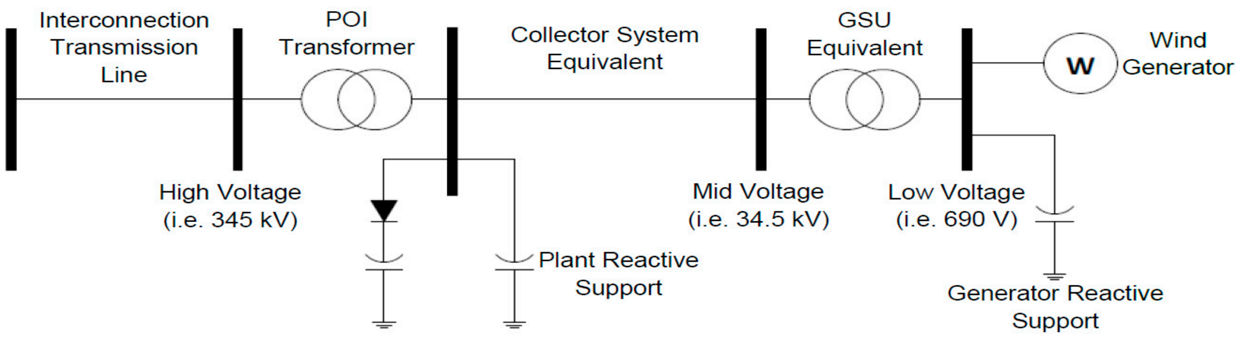

Figure 7. MISO renewable energy equivalent model [9,12].

Generator and transformer modeling considered the following factors.

- Modeling elements: control mode (power factor, voltage), power factor, reactive power supply range.
- Control mode modeling: modellable through WOD settings in PSS/E generators.

2.5. HVDC#3 Performance Analysis

HVDC#3 used in this paper was modeled with two types, the user-defined model UDM HVDC model and the generic model VSC model. The structure of the HVDC model was referred to through Appendix B. The VSC model was modeled in conjunction with the frequency controller.

As shown in Figure 8, it can be seen that the output of the UDM HVDC model changes quickly immediately after a system accident, the output fluctuation of the VSC model is smaller than that of the UDM HVDC model, and the output increases slowly. Due to such output characteristics, the two models also show different characteristics in frequency response characteristics.

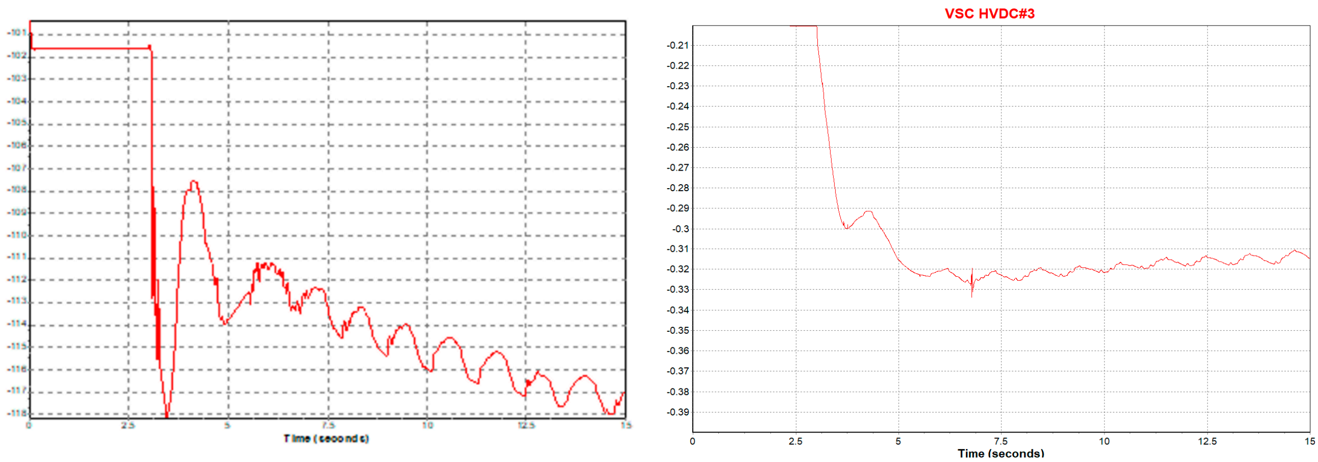

(**a**) (**b**)

Figure 8. Output characteristics by the HVDC model: (**a**) UDM HVDC Output characteristics and (**b**) VSC HVDC Output characteristics.

When comparing UDM HVDC modeling and VSC modeling, the lowest frequency of the UDM HVDC model was high, and there was a difference in the frequency waveform characteristics during the frequency recovery process.

3. Case Study

As shown in Figure 9, In the case study of this paper, the frequency response was analyzed according to the HVDC No.3 model, changing the ESS No.2 control mode and parameters. Because the frequency contribution to the UDM HVDC model was greater than that of the VSC model, the analysis was focused on the VSC model. Dynamic simulations for generator dropout accidents and three-phase short circuit accidents were run for all scenarios. Following the simulation, the optimal parameters of ESS No.2 were determined using a characteristic analysis for each parameter change, and the effect of changing the parameters was evaluated by comparing the optimal parameters, before and after they were applied. The frequency response characteristics according to each parameter change were referred to through the figure in Appendix A.

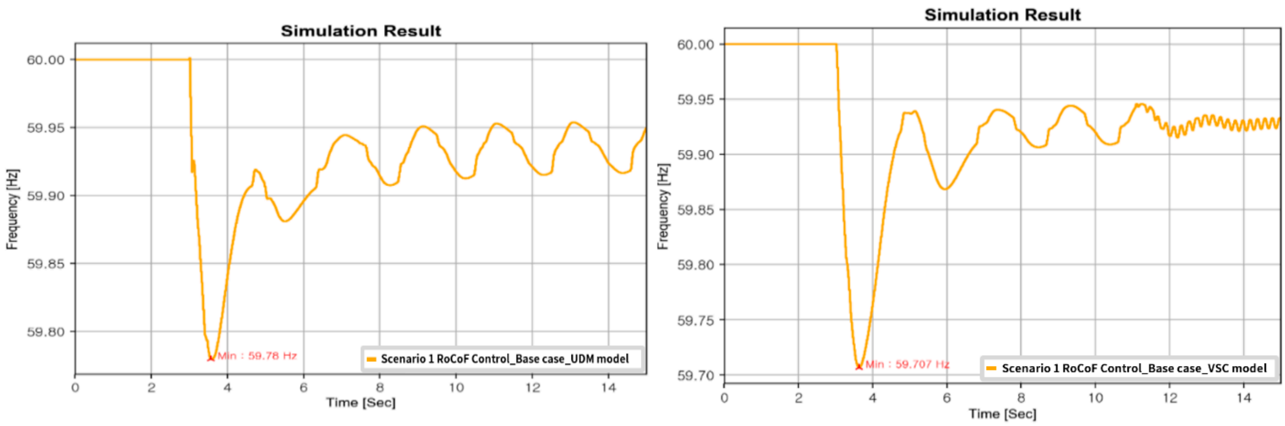

Figure 9. Frequency response characteristics by the HVDC model: UDM HVDC (**left**) and VSC HVDC (**right**).

3.1. Scenario A

Table 6 shows the characteristics of scenario A. Scenario A is classified according to the operation characteristics of HVDC No.1 and 2, and the DB was composed according to the renewable energy capacity and central power supply ratio. The frequency stability simulation was conducted by changing parameters according to the control mode (Droop, RoCoF) of the ESS.

Table 6. Scenario A configuration (HVDC No.3 non-modeling).

	Scenario 1	**Scenario 2**	**Scenario 3**	**Scenario 4**	**Scenario 5**
Characteristic	Non Renewable HVDC No.1,2 Supply	Much Renewable HVDC No.1,2 Supply	Middle Renewable HVDC No.1,2 Circulation	Few Renewable HVDC No.1,2 Circulation	Few Renewable HVDC No.1,2 Circulation

Table 7 shows the results of the lowest frequency according to the change of the ESS droop control parameter in scenario A. Given that the existing ESS speed adjustment rate was 0.33%, the effect of increasing the minimum frequency in response to a change in the speed adjustment rate was minimal. When the speed adjustment rate was set to 0.2%, the lowest frequency increased slightly, but the same result was observed in the majority of scenarios. In particular, in the case of a three-phase short circuit accident, the effect of increasing the frequency through the change of the speed adjustment ratio was small.

Table 7. Lowest frequency per parameter (droop control) (Hz): three-phase short circuit.

Scenario	**Base Case (0.33%)**	**Droop Speed**		
		0.2%	**0.3%**	**0.5%**
1	59.75 (59.64)	59.76 (59.64)	59.76 (59.64)	59.73 (59.64)
2	59.69 (59.42)	59.70 (59.43)	59.69 (59.42)	59.67 (59.41)
3	59.81 (59.56)	59.82 (59.57)	59.81 (59.57)	59.81 (59.57)
4	59.87 (58.99)	59.89 (59.19)	59.87 (59.74)	59.85 (59.61)
5	59.79 (59.50)	59.80 (59.50)	59.79 (59.50)	59.76 (59.50)

Figure 10 shows the frequency response waveform for each scenario. In the case of a three-phase short circuit, the frequency response waveform, including the lowest frequency, differed only slightly from the generator dropout accident. When the speed adjustment rate was reduced to 0.2% in the event of a generator dropout accident, the lowest frequency and settling frequency both increased, indicating that overall frequency stability improved.

As shown in Table 8, In the case of RoCoF control, modifiable parameters increased compared to the droop control, and stability, according to the transient judgment slope, normal/exit speed adjustment rate, and transient system constant fluctuations, were simulated. The simulation revealed that the change according to the transient judgment slope and speed adjustment rate was small and that as the transient system constant increased, the minimum frequency increased as the ESS output increased to the maximum output.

Regarding the three-phase short circuit, the lowest frequency decreased compared to the generator dropout accident, and the frequency increase effect due to transient system constant fluctuations also decreased. As shown in Figure 11, In scenario 2, as the proportion of renewable energy increased and the proportion of central power supply decreased, the lowest frequency was the lowest for both generator dropout and the three-phase short circuit when compared to other scenarios.

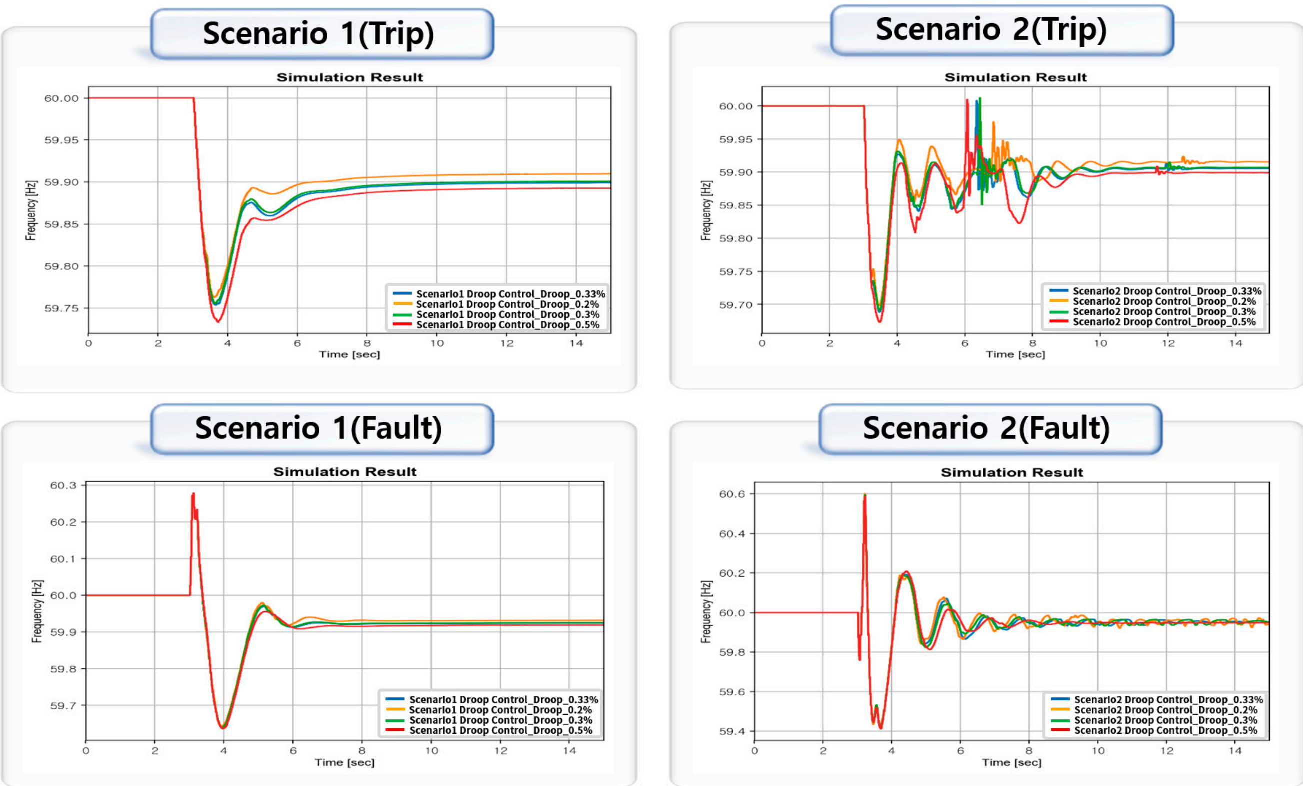

Figure 10. Frequency response by the ESS parameter (droop control).

Table 8. Lowest frequency per parameter (RoCoF Control) (Hz): three-phase short circuit.

Scenario	Base Case	RoCoF		Droop Speed		System H	
		0.05	0.1	0.5	1.0	200	300
1	59.71 (59.62)	59.71 (59.62)	59.71 (59.62)	59.71 (59.62)	59.71 (59.63)	59.75 (59.64)	59.76 (59.64)
2	59.64 (59.42)	59.64 (59.42)	59.64 (59.42)	59.63 (59.42)	59.63 (59.41)	59.68 (59.42)	59.70 (59.42)
3	59.79 (59.57)	59.79 (59.57)	59.79 (59.57)	59.79 (59.56)	59.79 (59.56)	59.82 (59.57)	59.82 (59.57)
4	59.84 (59.64)	59.84 (59.64)	59.84 (59.64)	59.84 (59.60)	59.85 (59.59)	59.87 (59.64)	59.88 (59.65)
5	59.74 (59.49)	59.74 (59.49)	59.74 (59.49)	59.74 (59.49)	59.73 (59.49)	59.77 (59.50)	59.78 (59.50)

3.2. Scenario B

As shown in Table 9, Scenario B is classified according to the UDM HVDC model and the generic model according to the forwarding operation of HVDC No.3 the DB was configured according to the renewable capacity and the central power supply ratio. Frequency stability simulation was performed by changing parameters according to the control mode (droop, RoCoF control) of the ESS.

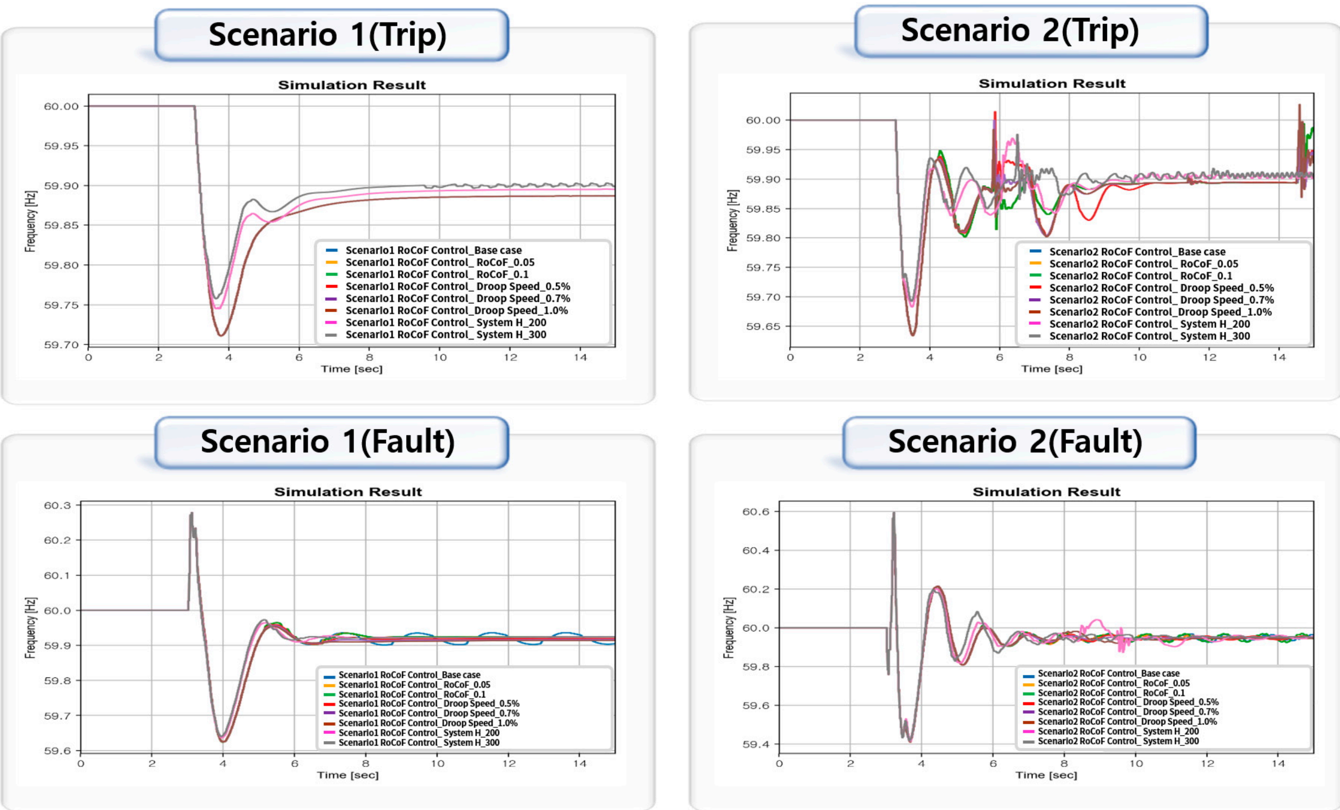

Figure 11. Frequency response by ESS parameter (RoCoF control).

Table 9. Scenario B configuration (HVDC#3 transmission).

	Scenario 1	Scenario 2	Scenario 3	Scenario 4	Scenario 5
Characteristic	Non Renewable HVDC No.1,2 Supply	Much Renewable HVDC No.1,2 Supply	Middle Renewable HVDC No.1,2 Circulation	Few Renewable HVDC No.1,2 Circulation	Middle Renewable HVDC No.1,2 Supply
	HVDC#3 VSC Model including Frequency Controller (Supply)				

Table 10 shows the lowest frequency results according to the ESS droop control parameter change in scenario B. As in scenario A, the effect of increasing the lowest frequency in response to a change in the speed adjustment rate was minimal. The lowest frequency increased slightly when the speed adjustment rate was set to 0.2%, but scenario B did not show the same large effect in most scenarios. The three-phase short circuit accident was also a starting point, and the effect of increasing the frequency by changing the speed adjustment rate was minor.

Table 10. Lowest frequency per parameter (droop control) (Hz): three-phase short circuit.

Scenario	Base Case (0.33%)	Droop Speed		
		0.2%	0.3%	0.5%
1	59.74 (59.58)	59.75 (59.58)	59.74 (59.58)	59.73 (59.58)
2	59.71 (59.62)	59.72 (59.61)	59.71 (59.62)	59.69 (59.63)
3	59.84 (59.66)	59.85 (59.65)	59.85 (59.66)	59.82 (59.67)

Table 10. *Cont.*

Scenario	Base Case (0.33%)	Droop Speed		
		0.2%	0.3%	0.5%
4	59.81 (59.59)	59.83 (59.58)	59.81 (59.58)	59.81 (59.59)
5	59.69 (59.78)	59.70 (59.78)	59.69 (59.78)	59.67 (59.78)

Figure 12 shows the frequency response result to the change of the ESS droop control parameter in Scenario B. Oscillation occurs during the frequency recovery process in scenario 3 due to the cyclic operation of HVDC, and, as in Scenario A, charging and discharging are repeated in the ESS exit control section, resulting in unstable stability.

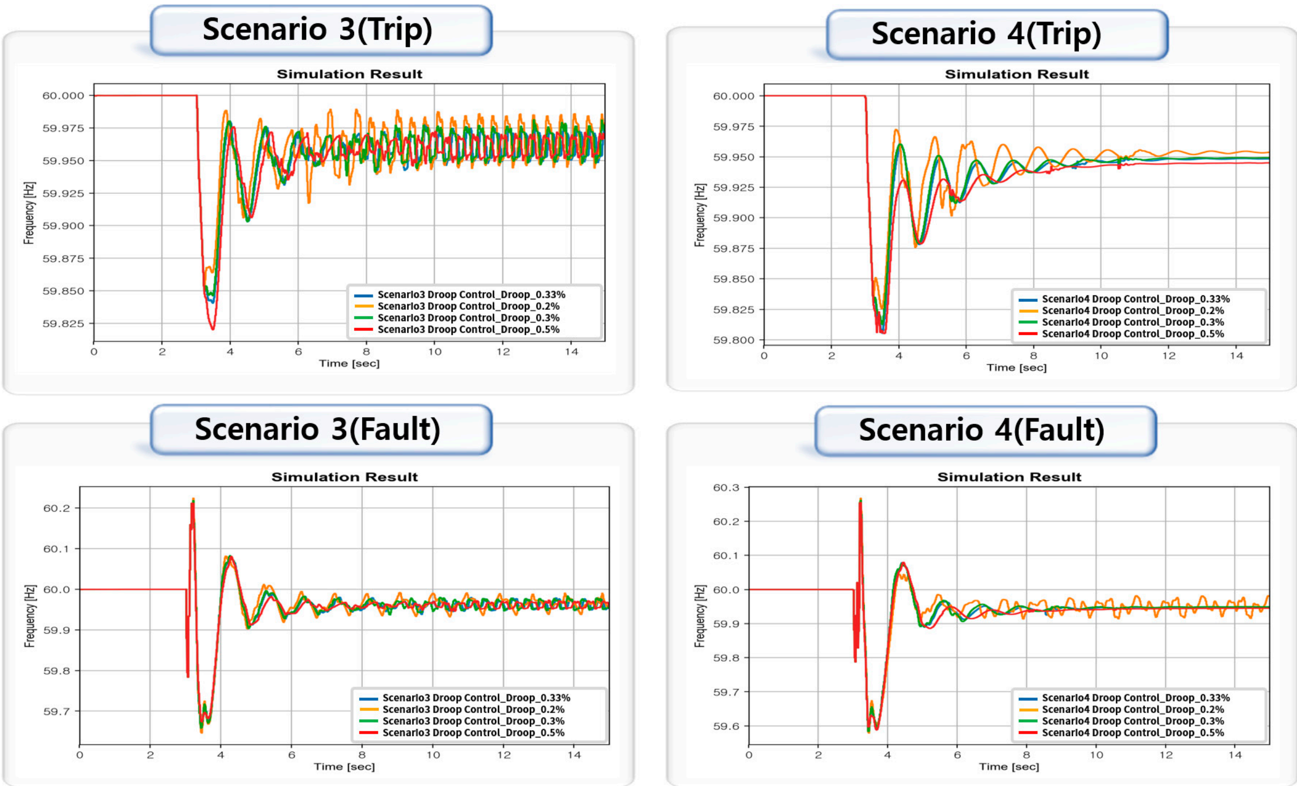

Figure 12. Frequency response by ESS parameter (droop control).

Similar to scenario A of the RoCoF control, the stability simulation was performed according to transient judgment slope, normal/exit speed adjustment rate, and transient system constant change. As shown in Table 11, In the case of a generator dropout accident, the improvement of stability through the transient system constant had a greater effect in Scenario 5 than in other scenarios.

Table 11. Lowest frequency per parameter (RoCoF Control) (Hz): three-phase short circuit.

Scenario	Base Case	RoCoF		Droop Speed		System H	
		0.05	0.1	0.5	1.0	200	300
1	59.71 (59.57)	59.71 (59.57)	59.71 (59.57)	59.71 (59.57)	59.71 (59.57)	59.73 (59.58)	59.75 (59.58)
2	59.66 (59.65)	59.66 (59.65)	59.66 (59.65)	59.66 (59.65)	59.66 (59.65)	59.70 (59.62)	59.71 (59.61)

Table 11. *Cont.*

Scenario	Base Case	RoCoF		Droop Speed		System H	
		0.05	0.1	0.5	1.0	200	300
3	59.80 (59.66)	59.80 (59.66)	59.80 (59.66)	59.80 (59.66)	59.80 (59.66)	59.83 (59.67)	59.85 (59.65)
4	59.79 (59.57)	59.79 (59.57)	59.79 (59.57)	59.79 (59.57)	59.79 (59.57)	59.81 (59.59)	59.82 (59.58)
5	59.63 (59.78)	59.63 (59.78)	59.63 (59.78)	59.63 (59.78)	59.63 (59.78)	59.68 (59.78)	59.69 (59.78)

Figure 13 shows the scenario 3 frequency response of scenario B. Oscillation occurs in the same way as in scenario A, and it is necessary to improve frequency stability through parameter adjustments.

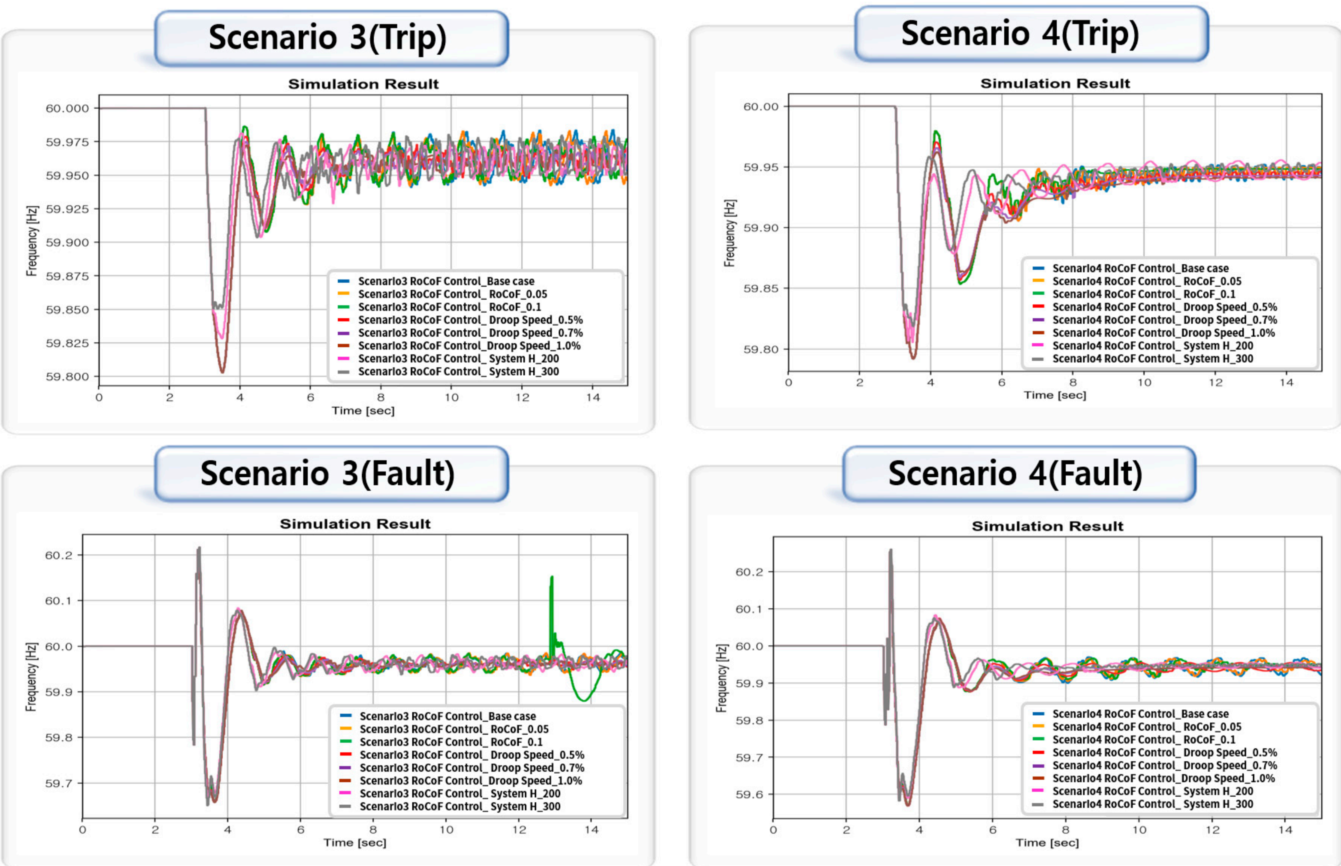

Figure 13. Frequency response by ESS parameter (RoCoF control).

As shown in the frequency response waveform, hunting increased during the frequency recovery process compared to scenario A. When the transient system constant increased, the lowest frequency showed an effect, and the three-phase short circuit did not show as much of a difference as the previous simulation results.

3.3. Scenario C

As shown in Table 12, Scenario C was modeled as a back-feeding operation of HVDC No.3, and the DB was configured according to the renewable capacity and central power supply ratio. As in the previous scenario, the frequency stability simulation was carried out by changing parameters based on the ESS control mode (droop, RoCoF). As shown in

Table 13, When the speed adjustment rate increased by 0.2%, scenario C had the same effect as scenarios A and B, and the three-phase short circuit had little effect. In scenarios 4 and 5, the frequency increase was greater than in the other cases.

Table 12. Scenario C configuration (HVDC No.3 transmission).

	Scenario 1	Scenario 2	Scenario 3	Scenario 4	Scenario 5
Characteristic	Non Renewable HVDC No.1,2 Supply	Much Renewable HVDC No.1,2 Supply	Middle Renewable HVDC No.1,2 Circulation	Few Renewable HVDC No.1,2 Circulation	Few Renewable HVDC No.1,2 Circulation
	HVDC No.3 VSC Model including Frequency Controller (Transmission)				

Table 13. Lowest frequency per parameter (droop control) (Hz): three-phase short circuit.

Scenario	Base Case (0.33%)	Droop Speed		
		0.2%	0.3%	0.5%
1	59.77 (59.64)	59.78 (59.64)	59.77 (59.64)	59.76 (59.64)
2	59.70 (59.45)	59.71 (59.45)	59.70 (59.45)	59.69 (59.45)
3	59.84 (59.50)	59.85 (59.49)	59.85 (59.49)	59.82 (59.51)
4	59.67 (59.31)	59.68 (59.31)	59.67 (59.31)	59.65 (59.32)
5	59.68 (59.36)	59.70 (59.36)	59.69 (59.36)	59.67 (59.36)

As shown in Figure 14, Scenario C had the same effect as scenarios A and B when changing the speed adjustment rate by 0.2%, and the three-phase short circuit had little effect. In the case of scenarios 4 and 5, the frequency increase increased compared to other cases.

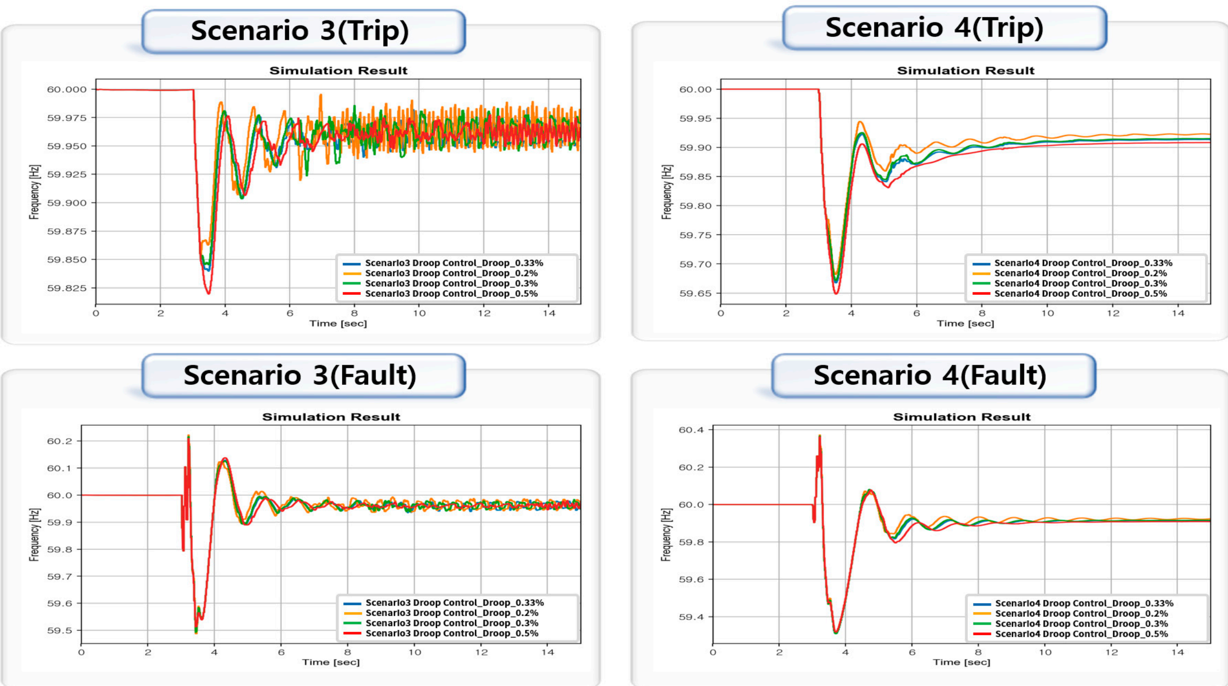

Figure 14. Frequency response by ESS parameter (droop control).

As shown in Table 14, In RoCoF control, as in the previous scenario, as the transient system constant increased, the lowest frequency improved, and in some cases of three-phase short circuits, the lowest frequency decreased. When the UDM model and the generic model were compared, the generic model had a higher lowest frequency, and both models had the same minimum frequency rise.

Table 14. Lowest frequency per parameter (RoCoF control) (Hz): three-phase short circuit.

Scenario	Base Case	RoCoF		Droop Speed		System H	
		0.05	0.1	0.5	1.0	200	300
1	59.74 (59.62)	59.74 (59.62)	59.74 (59.62)	59.74 (59.62)	59.74 (59.62)	59.76 (59.64)	59.78 (59.64)
2	59.65 (59.47)	59.65 (59.47)	59.65 (59.47)	59.65 (59.47)	59.65 (59.46)	59.70 (59.45)	59.70 (59.44)
3	59.80 (59.51)	59.80 (59.51)	59.80 (59.51)	59.80 (59.52)	59.80 (59.52)	59.83 (59.50)	59.85 (59.49)
4	59.61 (59.34)	59.61 (59.34)	59.61 (59.34)	59.61 (59.33)	59.61 (59.33)	59.66 (59.31)	59.67 (59.31)
5	59.63 (59.36)	59.63 (59.36)	59.63 (59.36)	59.62 (59.36)	59.62 (59.36)	59.68 (59.36)	59.69 (59.36)

As a result of the simulation, the lowest frequency increased due to ESS input, but it was unstable in the frequency recovery process, and the waveform showed unstable characteristics according to the operation characteristics of HVDC. Because the Jeju grid is small, the supply of active power via HVDC had a significant impact on frequency stability. As control strategies for improving frequency stability, ESS output power increase, droop speed increase, and dead band decrease were considered in a trans-state to increase the frequency nadir immediately after an accident. However, in the case of the droop speed increase and the dead band decrease, the frequency response showed instability, so that the charging and discharging states of the ESS were not repeated through the dead band increase. In addition, the parameter was selected, focusing on stabilization in the frequency recovery process by preventing a sudden change in frequency through a droop speed reduction in the exit control section. Based on these results, The optimal parameter setting was set as a parameter for cooperation between ESS No.1 and ESS No.2 to prevent frequency response oscillation that occurs when ESS No.2 is input, to improve the lowest frequency, and to ensure frequency stability. As illustrated in Figure 15, the instability caused by the frequency recovery process was reduced by adjusting the wide dead band and exit control. The optimal parameter was applied as follows.

- Dead band: $\pm$0.066 Hz;
- RoCoF for trans-state: 0.2 Hz/s;
- Droop speed (trans-recovery): 0.66%;
- System H for trans-state (ESS output).
- ESS#1: steady-state/exit control section quick response, fast exit control.
- ESS#2: fast response in case of transient response, accurate exit control.
- Maintenance, wide dead band.

When both ESS No.1 and No.2 showed excessive output in the exit control section, oscillation occurred during the frequency recovery process; this was compensated for. As shown in Figure 16, Charge/discharge according to frequency response was minimized by ESS No.2's wide dead band to ensure accurate exit control. It was designed to last. Tables 15 and 16 show the lowest frequencies of scenarios B and C before and after the ESS (RoCoF control) optimal parameter was applied. Although the lowest frequency was improved when applied optimally, the effect of parameters on frequency stability in the case of a three-phase short circuit was small, as shown in previous simulation results.

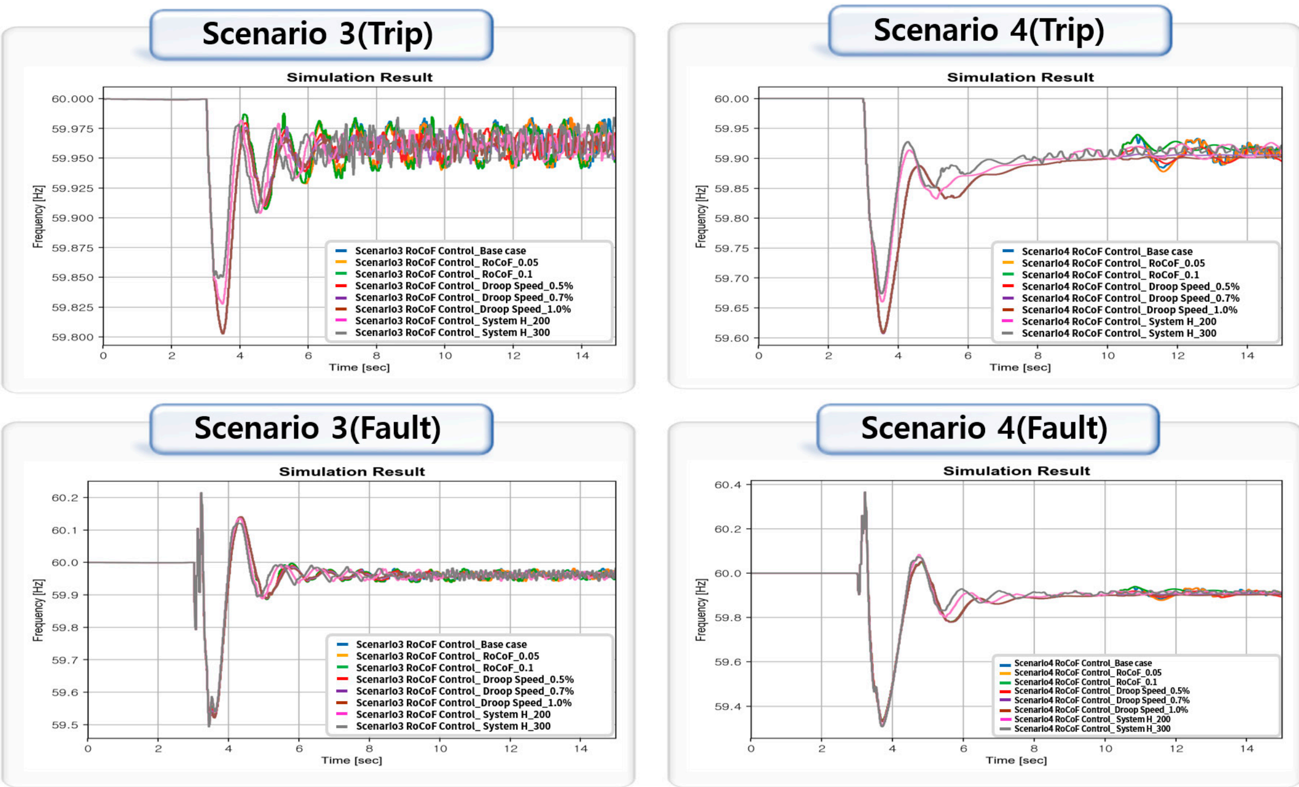

Figure 15. Frequency Response by ESS Parameter (RoCoF Control).

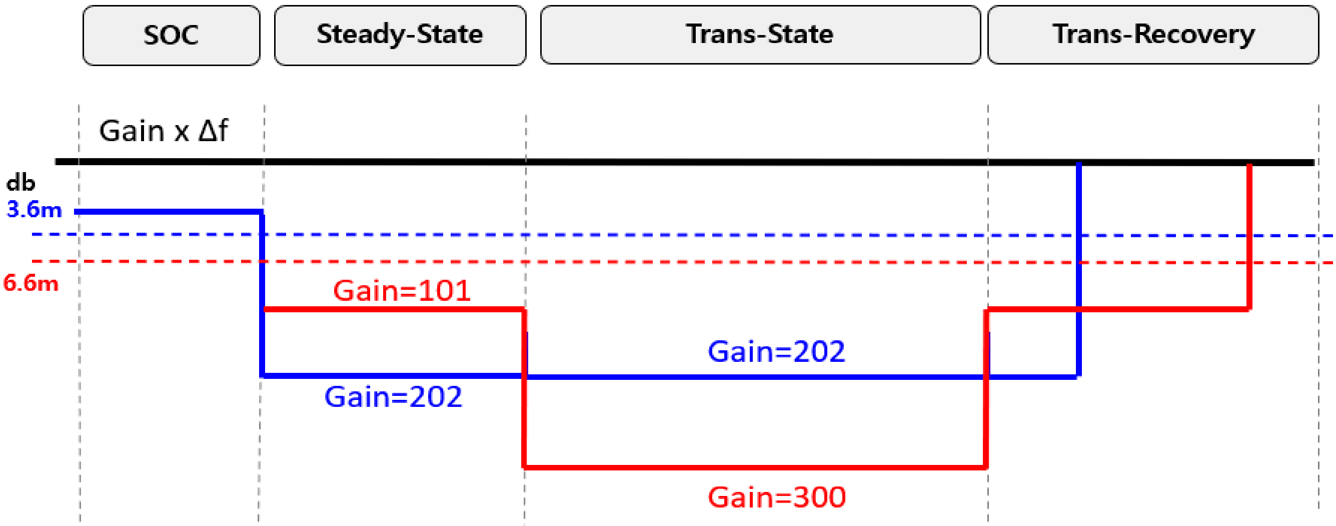

Figure 16. ESS operation strategy.

Table 15. Lowest frequency applying optimal parameters (generator trip) (Hz): before.

	Scenario 1	Scenario 2	Scenario 3	Scenario 4	Scenario 5
Scenario B	59.74 (59.71)	59.71 (59.66)	59.84 (59.80)	59.82 (59.79)	59.69 (59.63)
Scenario C	59.77 (59.74)	59.70 (59.65)	59.82 (59.80)	59.67 (59.61)	59.68 (59.63)

Table 16. Lowest frequency applying optimal parameters (three-phase short circuit) (Hz): before.

	Scenario 1	Scenario 2	Scenario 3	Scenario 4	Scenario 5
Scenario B	59.58 (59.57)	59.66 (59.65)	59.66 (59.66)	59.57 (59.57)	59.78 (59.78)
Scenario C	59.64 (59.62)	59.48 (59.47)	59.52 (59.51)	59.34 (59.34)	59.36 (59.36)

As a result of applying the ESS No.2 optimal parameter, the effect of improving the lowest frequency and instability in the frequency recovery process were resolved, as shown in Figure 17.

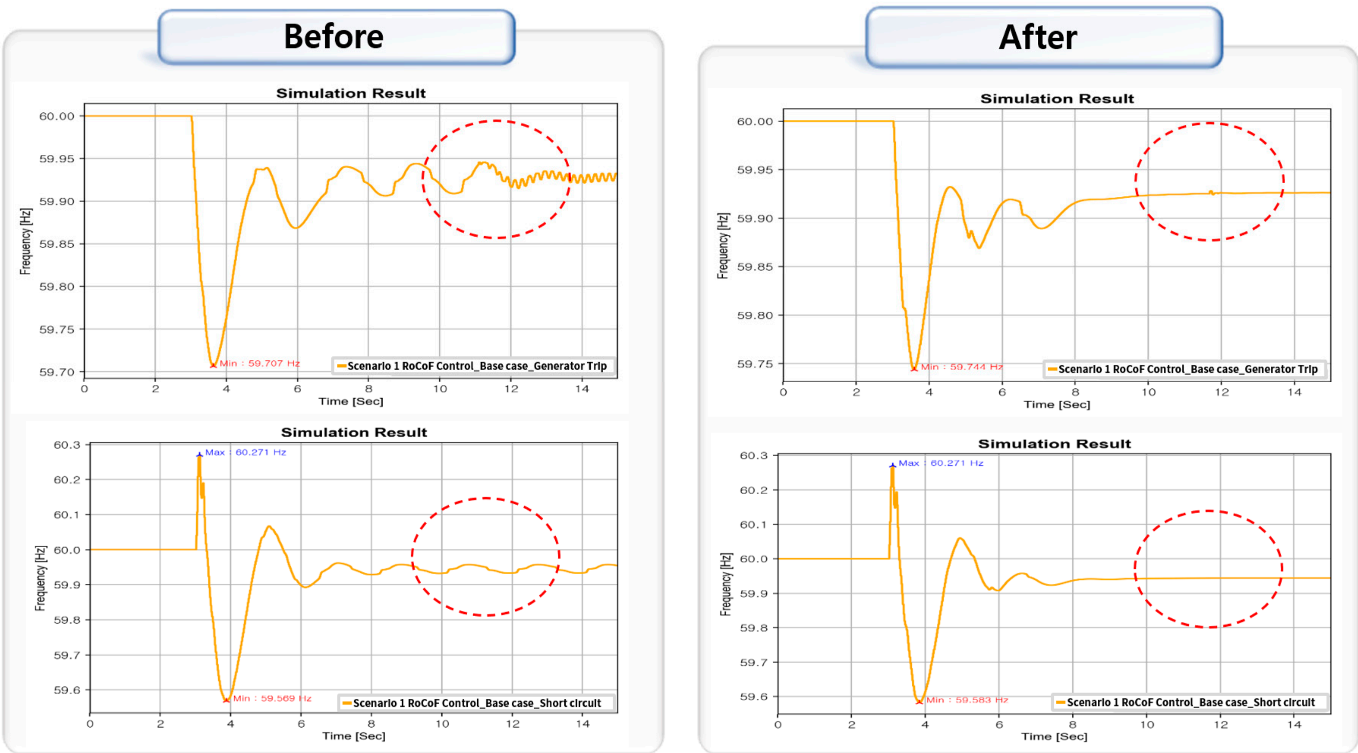

Figure 17. Effect of applying the ESS No.2 parameters.

When compared to the RoCoF control, droop control has fewer parameters that can be adjusted; even when the lowest frequency is improved via the transient system constant, instability may appear during the frequency recovery process. However, if the exit control section's speed adjustment rate can be adjusted for a stable frequency response while minimizing the occurrence of oscillation during the frequency recovery process, frequency stability will be improved over the current state.

Figures 18 and 19 show the wind power generator output based on the ESS output and frequency response characteristics before and after the optimal parameter application. With the application of the optimal parameters, the ESS output power was stabilized, and the wind generator output showed a stable output power, even though oscillation occurred in some parts due to frequency fluctuations.

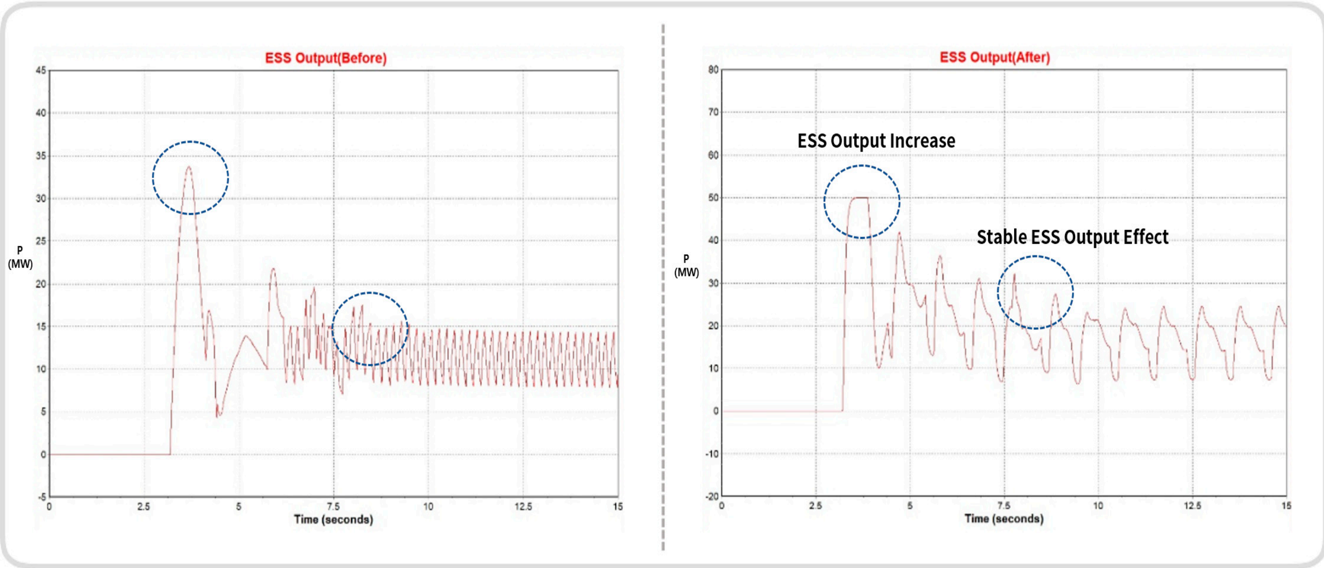

Figure 18. Comparison of ESS output before and after applying optimal parameters.

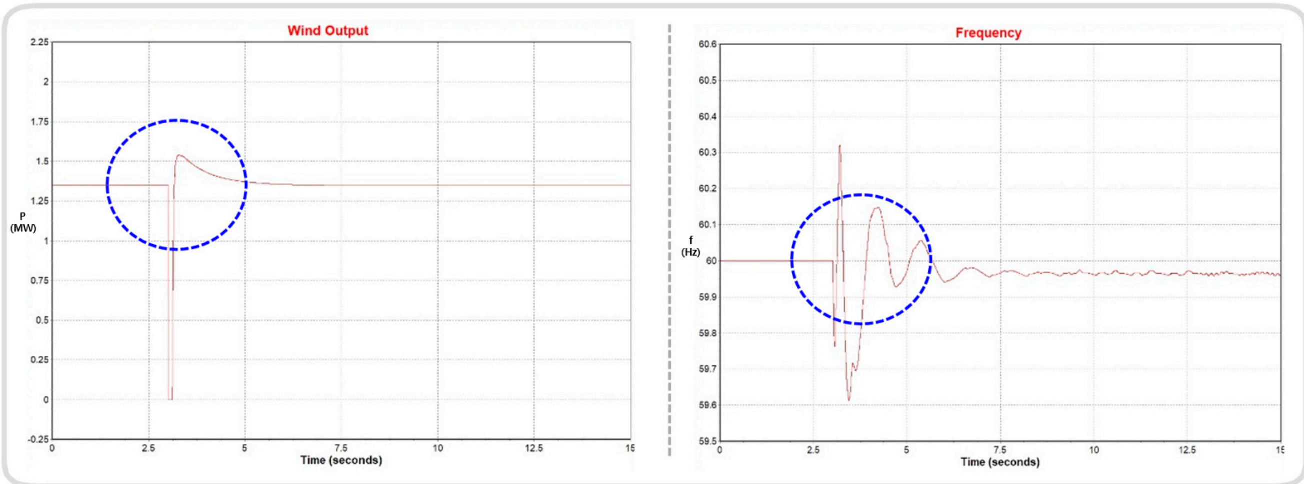

Figure 19. Comparison of wind power generator output characteristics according to frequency response characteristics.

4. Conclusions

The output of the ESS was stabilized during the frequency recovery process as the dead band was widened, the exit control speed adjustment rate was adjusted, and the oscillation that previously occurred due to the repeated charging and discharging states was reduced.

In this paper, to improve the frequency stability of the inverter-based Jeju grid, the lowest frequency improvement and stable frequency response were simulated by changing the parameters and control mode of the ESS. The effectiveness of the method for reducing frequency response oscillation by adjusting the dead band and droop and improving the lowest frequency by increasing the system H was confirmed by this paper. In the case of System H, it was effective at improving the lowest frequency via a full-discharge in the transient section, but there was a limit based on the ESS capacity. Because the Jeju grid was small, frequency response oscillation occurred when excessive discharge occurred while securing frequency stability via ESS. To prevent this, the dead band's range must be expanded. Furthermore, the ESS output must be stabilized by adjusting the droop of the exit control section. The parameter setting used in this paper has the effect of increasing the utilization of the ESS and improving the lowest frequency by increasing the

ESS output. Moreover, by adjusting the droop speed to have a quick response characteristic, by widening the dead band to minimize the charge and discharge of the ESS, and to enable stable output, the result was shown to minimize the oscillation generated in the frequency recovery process. In the case of a small-scale power system, the frequency response characteristics are greatly changed according to small elements of the system. In order to improve the frequency stability of a small-scale power system, detailed system adjustments are required; this is the same in the ESS operation plan. The change of the ESS parameter used in this paper shows the effect of improving the stable output of the ESS and reducing the oscillation in the frequency recovery process at the lowest frequency. The parameter setting in this paper will have a great effect on the ESS operation plan and control strategy of small-scale power systems, including the Jeju power system.

As the Jeju grid is a small-scale system, frequency fluctuations will be evident due to changes in ESS parameters. Unlike previous papers, this paper analyzed the frequency stabilization effect of ESS through various parameter changes, such as ESS control mode and droop speed. Moreover, the frequency nadir increased as well as the stabilization in the frequency recovery process; thus, it can be used as a method to operate ESS to contribute to the stable power output and frequency stabilization of ESS.

In future research, we intend to study the frequency stability improvement effect and operation strategy of ESS in a large-scale system rather than a small-scale system, such as the Jeju grid. A large number of ESS are connected to a large-scale power system. As a large amount of money is invested in ESS power system connections, it should be used in various ways for economic benefits. ESS can also be effective at easing power generation constraints, including frequency recovery, and show higher efficiency through control strategies [13]. As the number of renewable generators increases in future systems along with ESS, it is necessary to consider ways to improve the stability of the power system through the control strategy of renewable generators [14]. In addition, as the supply of effective power through HVDC is important for the Jeju grid, additional research will be conducted according to the operating characteristics and effective power of HVDC.

Author Contributions: Conceptualization, Y.-S.C. and H.S.; methodology, J.-Y.J.; validation, Y.-S.C. and J.-Y.J.; formal analysis, Y.-S.C. and J.-Y.J.; investigation, J.-Y.J.; data curation, J.-H.M.; writing—original draft preparation, J.-Y.J.; writing—review and editing, Y.-S.C. and J.-Y.J.; visualization, Y.-S.C. and H.S.; supervision, Y.-S.C.; project administration, J.-H.M. All authors have read and agreed to the published version of the manuscript.

Funding: This research received no external funding.

Informed Consent Statement: Informed consent was obtained from all subjects involved in the study. And Written informed consent has been obtained from the patient(s) to publish this paper.

Acknowledgments: This work was supported by the Korea Electronic Power Corporation (KEPCO).

Conflicts of Interest: The authors declare no conflict of interest.

Abbreviations

ESS	energy storage system
PV	photovoltaics
RE	renewable energy
Gridpl	power system
PSH	pumped storage hydroelectricity
HVDC	high voltage direct current
FFR	fast frequency response
PFR	primary frequency response
RoCoF	rate of change of frequency
UDM	user defined model
VSC	voltage source convertor
Trans-state	transient state

Steady-state	stationary state/steady state
Trans-recovery	transient recovery state
SOC	state of charge
WECC	western electricity coordinating council
Trip	generator trip
Fault	three-phase short circuit

Appendix A

Figures A1–A3 shows the frequency response characteristics according to ESS parameter changes. The frequency nadir increased in some cases when adjusting RoCoF for trans-state, but in most cases the effects were small.

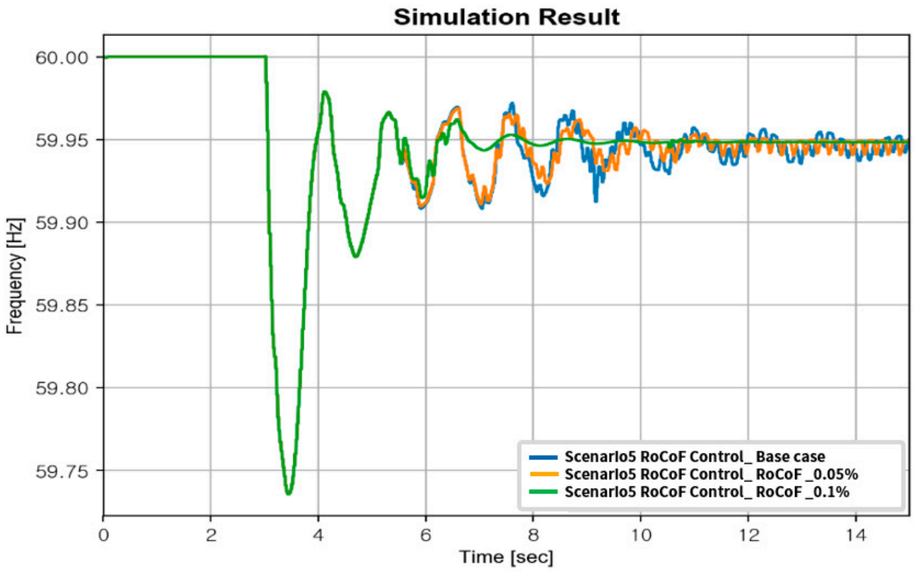

Figure A1. Frequency response by ESS parameter (RoCoF for trans-state).

During the droop speed adjustment, the faster the ESS operation was performed, the frequency nadir increase effect was shown, but oscillation occurred during the frequency recovery process. In addition, the slower the ESS operation through the droop speed adjustment, the lower the oscillation and the frequency stabilized.

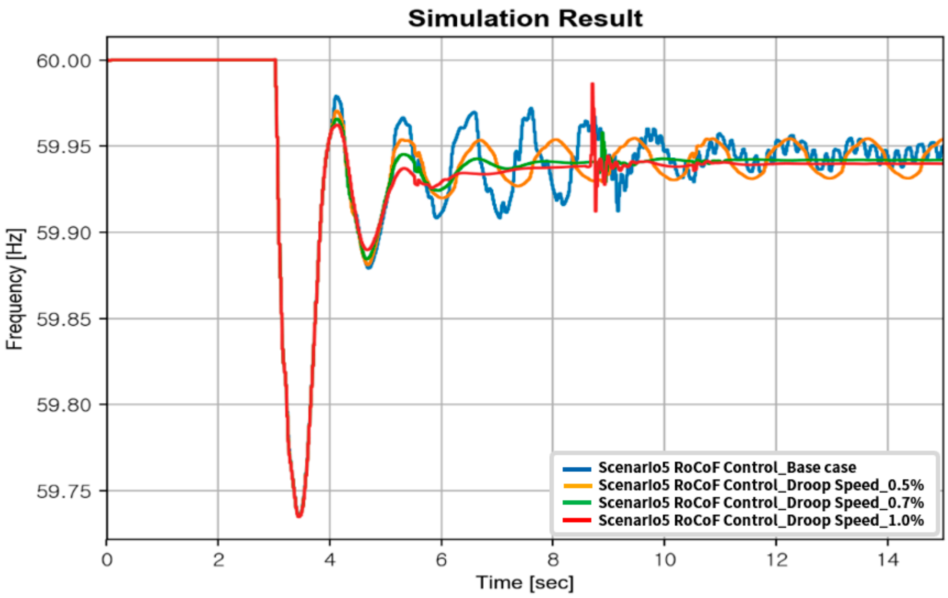

Figure A2. Frequency response by ESS parameter (droop speed).

When system H increased, the minimum frequency increased as the ESS output power increased in the trans-state, but oscillation occurred, as in the result of the droop speed adjustment.

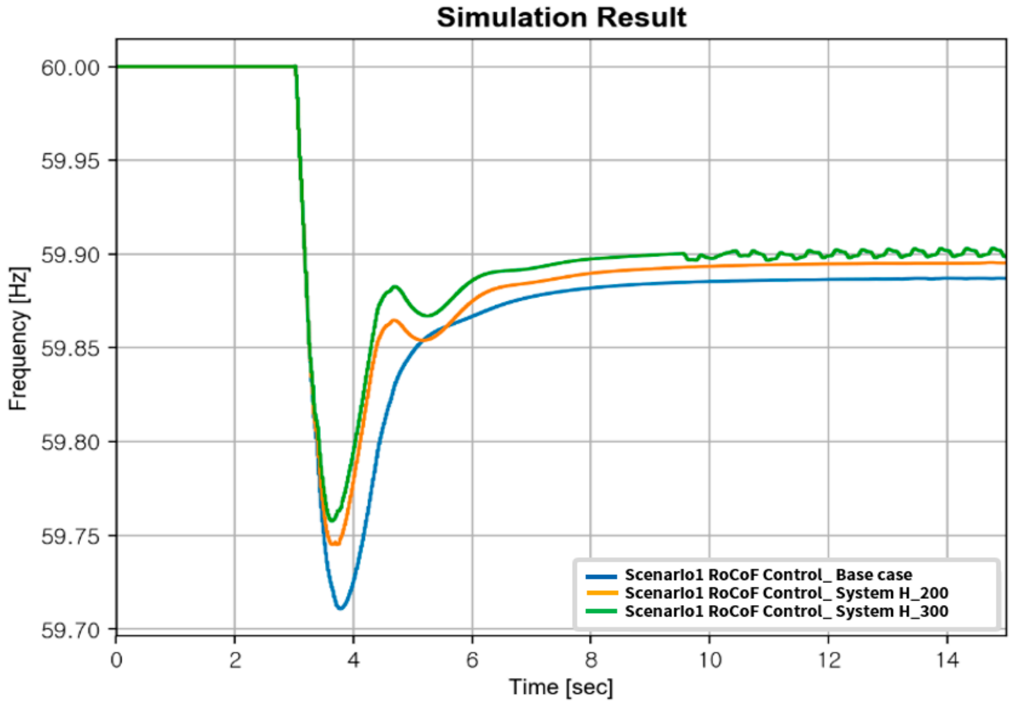

Figure A3. Frequency response by ESS parameter (system H (ESS output) for trans-state).

Appendix B

Figures A4–A6 show the mathematical models of renewable energy, HVDC, and ESS used in this paper's case study.

(1) Renewable energy.

This paper used a model provided by PSS/E, consisting of pitch control of REPCAU1, as shown in Figure A2.

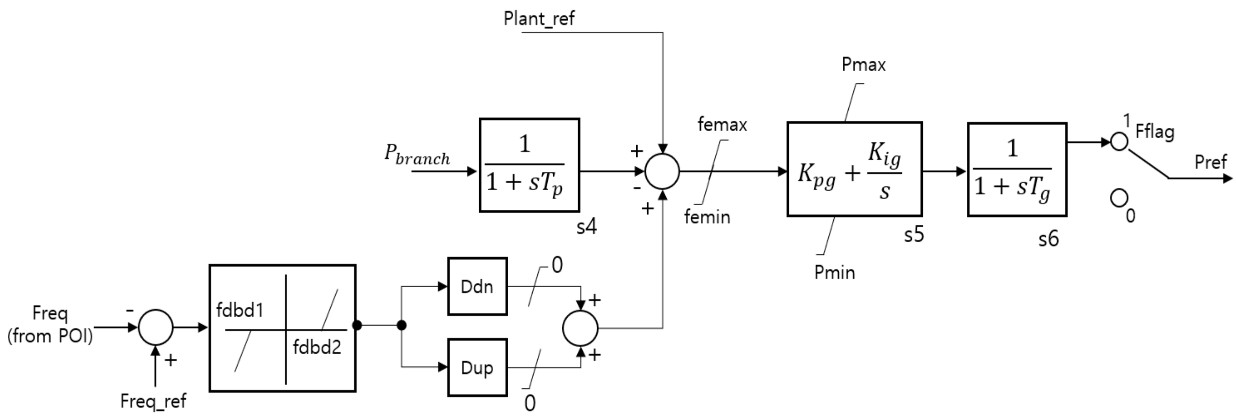

Figure A4. REPCAU1 model of PSS/E [15,16].

(2) HVDC.

The HVDC model in this paper used the model provided by PSS/E; it was configured, as shown in Figure A3.

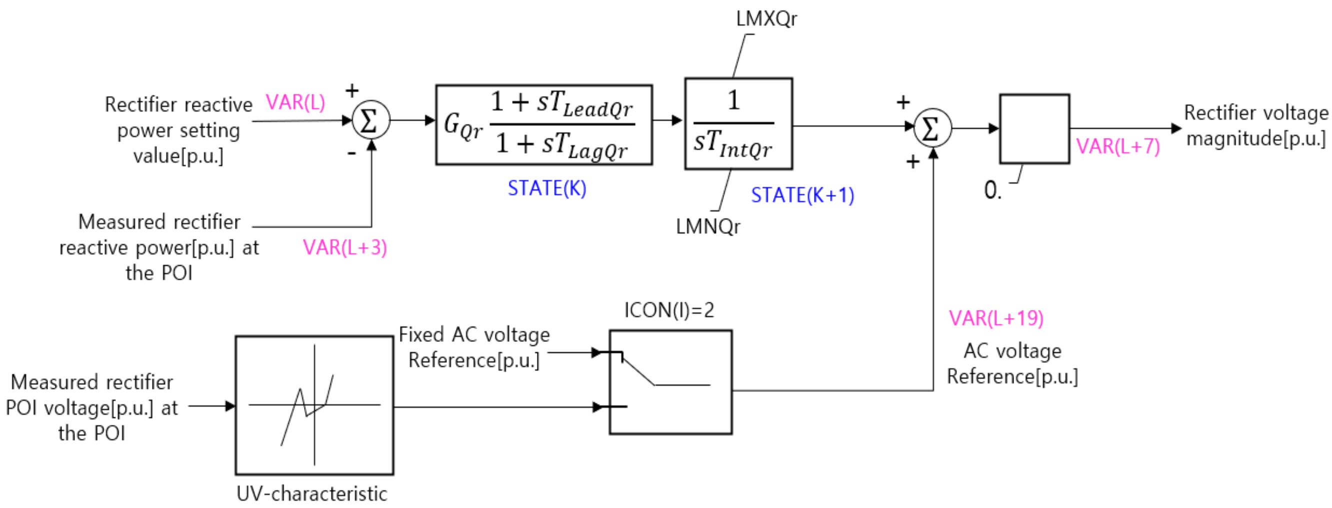

Figure A5. HVDCPLU1 model of PSS/E [15,16].

(3) Energy storage system(s) (ESS).

The ESS output of this paper determined the output through the following calculation. The output amount was calculated in consideration of frequency deviation and droop speed.

$$P = (60 - f_{meas}) \times \frac{M_{base}}{60 \times R_{ss}} \tag{A1}$$

$$\Delta f = 60 - f_{meas} \tag{A2}$$

$$R_{ss} = Droop\ Speed \tag{A3}$$

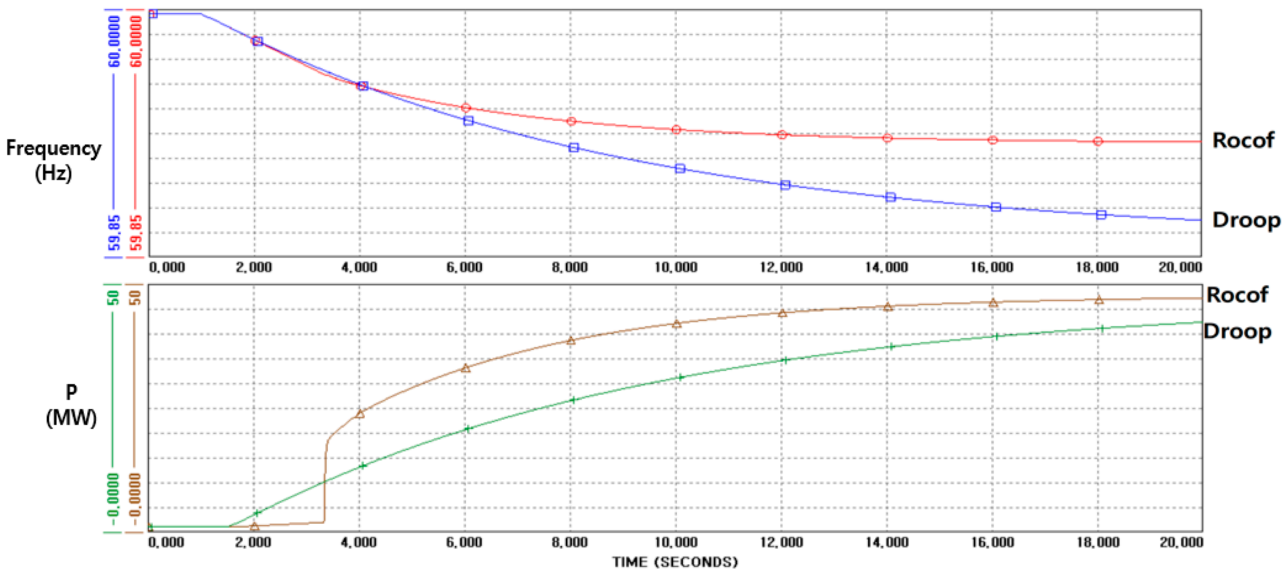

Figure A6. Examples of ESS output characteristics.

References

1. Ministry of Trade, Industry and Energy. *The 9th Basic Plan for Long-Term Electricity Supply and Demand*; Ministry of Trade, Industry and Energy: Sejong City, Korea, 2020.
2. ERCOT. *Inertia: Basic Concepts and Impacts on the ERCOT Grid*; ERCOT: Austin, TX, USA, 2018.

3. EIRGRID. *DS3 Programme Transition Plan*; EIRGRID and SONI: Ireland, Dublin, 2018.
4. ENTSO-E. *Nordic Report: Future System Inertia*; ENTSO-E: Brussels, Belgium, 2018.
5. Arévalo, P.; Tostado-Véliz, M.; Jurado, F. A novel methodology for comprehensive planning of battery storage systems. *J. Energy Storage* **2021**, *37*, 102456. [CrossRef]
6. MISO. *Renewable Integration Impact Assessment*; MISO: Carmel, IN, USA, 2018.
7. NERC. *Fast Frequency Response Concepts and Bulk Power System Reliability Needs*; NERC: Atlanta, GA, USA, 2020.
8. Yoo, G.M. *The World of Electricity*; The Korean Institute of Electrical Engineers: Seoul, Korea, 2018.
9. Yoon, M.H.; Lee, J.H.; Song, S.Y.; Yoo, Y.T.; Jand, G.S.; Jung, S.M.; Hwand, S.C. Utilization of Energy Storage System for Frequency Regulation in Large-Scale Transmission System. *Energies* **2019**, *12*, 3898. [CrossRef]
10. Alves, E.F.; Mota, D.S.; Tedeschi, E. *Sizing of Hybrid Energy Storage Systems for Inertial and Primary Frequency Control*; Frontiers in Energy Research: Lausanne, Switzerland, 2021.
11. Kpoto, K.; Sharma, A.M.; Sharma, A. *Effect of Energy Storage System in Low Inertia Power System with High Renewable Energy Sources*; IEEE: New York, NY, USA, 2019.
12. MISO. *MISO MOD-032 Model Data Requirements & Reporting Procedures*; MISO: Carmel, IN, USA, 2015.
13. Zhao, B.; Wang, X.; Haessing, P. *A Novel SoC Feedback Control of ESS for Frequency Regulation of Fractional Frequency Transmission System with Offshore Wind Power*; IEEE: New York, NY, USA, 2017.
14. Denholm, P.L.; Sun, Y.; Mai, T.T. *An Introduction to Grid Services: Concepts, Technical Requirements, and Provision from Wind*; NREL: Golden, CO, USA, 2019.
15. SIEMENS. *PSS/E Model Library*; SIEMENS: Munich, Germany, 2018.
16. NERC. *Modeling Notification: Recommended Practices for Modeling Momentary Cessation*; NERC: Atlanta, GA, USA, 2018.